PHYSICAL REVIEW D **83,** 034031 (2011)

How perfect can a gluon plasma be in perturbative QCD?

Jiunn-Wei Chen,[1] Jian Deng,[2] Hui Dong,[2] and Qun Wang[3]

[1]*Department of Physics and Center for Theoretical Sciences, National Taiwan University, Taipei 10617, Taiwan*
[2]*School of Physics, Shandong University, Shandong 250100, People's Republic of China*
[3]*Interdisciplinary Center for Theoretical Study and Department of Modern Physics, University of Science and Technology of China, Anhui 230026, People's Republic of China*

(Received 18 November 2010; revised manuscript received 16 January 2011; published 23 February 2011)

The shear viscosity to entropy density ratio, η/s, characterizes how perfect a fluid is. We calculate the leading order η/s of a gluon plasma in perturbation using the kinetic theory. The leading order contribution only involves the elastic $gg \leftrightarrow gg$ (22) process and the inelastic $gg \leftrightarrow ggg$ (23) process. The hard-thermal-loop (HTL) treatment is used for the 22 matrix element, while the exact matrix element in vacuum is supplemented by the gluon Debye mass insertion for the 23 process. Also, the asymptotic mass is used for the external gluons in the kinetic theory. The errors from not implementing HTL and the Landau-Pomeranchuk-Migdal effect in the 23 process, and from the uncalculated higher order corrections, are estimated. Our result smoothly connects the two different approximations used by Arnold, Moore, and Yaffe (AMY) and Xu and Greiner (XG). At small α_s ($\alpha_s \ll 1$), our result is closer to AMY's collinear result while at larger α_s the finite angle noncollinear configurations become more important and our result is closer to XG's soft bremsstrahlung result. In the region where perturbation is reliable ($\alpha_s \lesssim 0.1$), we find no indication that the proposed perfect fluid limit $\eta/s \simeq 1/(4\pi)$ can be achieved by perturbative QCD alone. Whether this can be achieve for $\alpha_s \gtrsim 0.1$ is still an open question.

DOI: 10.1103/PhysRevD.83.034031 PACS numbers: 12.38.Mh

I. INTRODUCTION

A *perfect fluid* is a system with zero shear and bulk viscosities, η and ζ, and no dissipation. These conditions can be satisfied for a superfluid at zero temperature where only the superfluid component exists, but a sharper description is with the dimensionless ratios η/s and ζ/s, where s, the entropy density, vanishes for the superfluid component as well. While ζ/s can still be zero for scaling invariant systems, the situation for η/s is more subtle.

In general, stronger interactions implies a smaller η. Thus, a perfect fluid with the smallest η/s is likely to be strongly interacting, which requires nonperturbative tools to compute it. The anti-de Sitter space/conformal field theory correspondence (AdS/CFT) [1–3] allows the η/s of strongly interacting CFT's to be computed in weakly interacting gravitational theories. A universal number $\eta/s = 1/(4\pi)$ is found for every CFT with a gravity dual in the large N, with N the size of the gauge group, and infinite 't Hooft coupling limit [4–6]. With this result, together with the connection to the uncertainty principle through the relation $\eta/s \sim \Delta E \Delta t$, with ΔE and Δt the mean energy and lifetime of quasiparticles, Kovtun, Son, and Starinets (KSS) [5] conjectured that the strongly interacting CFT value $1/(4\pi)$ is the minimum bound for η/s for all physical systems.

Theoretically, there are several attempts to evade this bound. It is found that η/s can be as small as possible (but still non-negative) in a carefully engineered meson system [7,8], although the system is metstable. Also, in strongly interacting CFTs, $1/N$ corrections can be negative [9,10] and can modify the η/s bound slightly [11,12].

Experimentally, there are intensive interests to find the most perfect fluid (see [13,14] for recent reviews). The smallest η/s known so far is realized in a system of hot and dense matter thought to be quark-gluon plasma (QGP) just above the phase transition temperature produced at the Relativistic Heavy Ion Collider (RHIC) [15–17] with $\eta/s = 0.1 \pm 0.1(\text{theory}) \pm 0.08(\text{experiment})$ [18]. A robust upper limit $\eta/s < 5 \times 1/(4\pi)$ was extracted by another group [19] and a lattice computation of gluon plasma yields $\eta/s = 0.134(33)$ [20]. Progress has been made in cold unitary fermi gases as well. An analysis of the damping of collective oscillations gives $\eta/s \gtrsim 0.5$ [21,22]. Even smaller values of η/s are indicated by recent data on the expansion of rotating clouds [23,24], but more careful analyses are needed [25,26].

Even if the $1/(4\pi)$ bound for η/s turns out to be invalid, it is still interesting to use it as a benchmark value for the perfectness of fluids. It was found that based on the perturbative QCD (PQCD) analysis of Arnold, Moore and Yaffe (AMY) [27,28], the measured η/s at RHIC cannot be explained by PQCD (for a recent review, see, e.g., [29]). This strongly interacting QGP picture is very different from the conventional picture of weakly interacting QGP and is considered as one of the most surprising discoveries at the RHIC.

However, a recent perturbative QCD calculation of η/s of a gluon plasma by Xu and Greiner (XG) [30] shows that the dominant contribution comes from the inelastic $gg \leftrightarrow ggg$ (23) process instead of the elastic $gg \rightarrow gg$ (22) process. In particular, the 23 process is 7 times more important than 22. Thus, $\eta/s \simeq 1/4\pi$ can be achieved when the strong coupling constant $\alpha_s \simeq 0.6$. Thus, the

conventional weakly interacting QGP could still be valid. This is in sharp contrast to AMY's result, where the 23 process only gives $\sim 10\%$ correction to the 22 process.

Both XG and AMY use kinetic theory for their calculations. The main differences are (i) XG uses a parton cascade model [31] to solve the Boltzmann equation and, for technical reasons, gluons are treated as a classical gas instead of a bosonic gas. On the other hand, AMY solves the Boltzmann equation for a bosonic gas. (ii) AMY approximates the $Ng \leftrightarrow (N+1)g$ processes, $N = 2, 3, 4\ldots$, by the $g \leftrightarrow gg$ splitting in the collinear limit where the two gluon splitting angle is higher order. XG uses the soft gluon bremsstrahlung limit where one of the gluon momenta in the final state of $gg \rightarrow ggg$ is soft but it can have a large splitting angle with its mother gluon.

In an earlier attempt to resolve the discrepancy between XG's and AMY's results [32], a Boltzmann equation computation of η is carried out without taking the classical gluon approximation (like AMY's approach), but the soft gluon bremsstrahlung limit is applied to the 23 matrix element (like XG's approach, modulo a factor 2 in the 23 matrix element squared; see [32] for details). It was found that the classical gas approximation does not cause a significant error in η/s (although the individual errors on η and s are larger). However, the result is sensitive to whether the soft gluon bremsstrahlung limit is imposed on the phase space or not. If this limit is imposed, the result is closer to AMY's; if not, the result is closer to XG's. This raises the concern whether this approximation is good for computing η.

The goal of this paper is to settle this issue by removing both the soft gluon bremsstrahlung approximation and the collinear approximation to the 23 process. The leading order $[O(\alpha_s^{-2})]$ contribution to η only involves the 22 and 23 processes [28] (the power counting for 22, 23, and other processes are reproduced in [32]). In this paper, the Hard-Thermal-Loop (HTL) treatment is used for the 22 matrix element, while the exact matrix element in vacuum is supplemented by the gluon Debye mass insertion for the 23 process. Also, the Debye mass is used for the external gluon mass in the kinetic theory as well. The errors from not implementing HTL and the Landau-Pomeranchuk-Migdal effect in the 23 process, and from the uncalculated higher order corrections, are also estimated.

II. KINETIC THEORY BEYOND THE SOFT OR COLLINEAR GLUON APPROXIMATIONS

Using the Kubo formula, η can be calculated through the linearized response function of a thermal equilibrium state

$$\eta = -\frac{1}{5}\int_{-\infty}^{0} dt' \int_{-\infty}^{t'} dt \int dx^3 \langle [T^{ij}(0), T^{ij}(\mathbf{x}, t)]\rangle, \quad (1)$$

where T^{ij} is the spatial part of the off-diagonal energy momentum tensor. In a leading order (LO) expansion of the coupling constant, there are an infinite number of diagrams [33,34]. However, it is proven that the summation of the LO diagrams in a weakly-coupled ϕ^4 theory [33–37] or in hot QED [38] is equivalent to solving the linearized Boltzmann equation with temperature-dependent particle masses and scattering amplitudes. The conclusion is expected to hold in weakly-coupled systems and can as well be used to compute the LO transport coefficients in QCD-like theories [27,28], hadronic gases [39–44] and weakly-coupled scalar field theories [33–36,45,46].

The Boltzmann equation of a hot gluon plasma describes the evolution of the color and spin-averaged gluon distribution function $f_p(x)$, which is a function of space-time $x = (t, \mathbf{x})$ and momentum $p = (E_p, \mathbf{p})$. The infinitesimal deviation of $f_p(x)$ from its equilibrium value $f_p^{\rm eq} = (e^{v\cdot p/T} - 1)^{-1}$ is denoted as

$$f_p = f_p^{\rm eq}[1 - \chi_p(1 + f_p^{\rm eq})], \quad (2)$$

where $\chi_p \equiv \chi(x, p)$ can be parametrized as

$$\chi_p = \frac{A(p)}{T}\nabla\cdot\mathbf{v} + \frac{B_{ij}(p)}{T}\frac{1}{2}\left(\frac{\partial v^i}{\partial x^j} + \frac{\partial v^j}{\partial x^i} - \frac{2}{3}\delta_{ij}\nabla\cdot\mathbf{v}\right), \quad (3)$$

at the leading order of the derivative expansion of the fluid velocity $v(x) = (v^0, v)$. $T = T(x)$ is the local temperature, $\hat{\mathbf{p}}$ is the unit vector in the $\mathbf{p}$ direction. $B_{ij}(p) = B(p)\times(\hat{\mathbf{p}}^i\hat{\mathbf{p}}^j - \frac{1}{3}\delta_{ij})$. $A(p)$ and $B(p)$ are functions of $\mathbf{p}$ which will be fixed by the Boltzmann equation corresponding to the bulk and shear viscosities, respectively. In this work, we will just focus on the shear viscosity calculation.

The Boltzmann equation [47–52] for the gluon plasma reads

$$\begin{aligned}\frac{p^\mu}{E_p}\partial_\mu f_p = \frac{1}{N_g}\sum_{(n,l)}\frac{1}{N(n,l)}\int_{1\cdots(n-1)} d\Gamma_{1\cdots l\rightarrow(l+1)\cdots(n-1)p} \\ \times\Bigg[(1+f_p)\prod_{r=1}^{l} f_r \prod_{s=l+1}^{n-1}(1+f_s) \\ - f_p\prod_{r=1}^{l}(1+f_r)\prod_{s=l+1}^{n-1} f_s\Bigg],\end{aligned} \quad (4)$$

where the collision rates are given by

$$\begin{aligned}&d\Gamma_{1\cdots l\rightarrow(l+1)\cdots(n-1)p} \\ &\equiv \prod_{j=1}^{n-1}\frac{d^3\mathbf{p}_j}{(2\pi)^3 2E_j}\frac{1}{2E_p}|M_{1\cdots l\rightarrow(l+1)\cdots(n-1)p}|^2 \\ &\times(2\pi)^4\delta^4\left(\sum_{r=1}^{l} p_r - \sum_{s=l+1}^{n-1} p_s - p\right).\end{aligned} \quad (5)$$

$N_g = 16$ is the color and spin degeneracy of a gluon. The i-th gluon is labeled as i, while the n-th gluon is labeled as p. For a process with l initial and $(n-l)$ final gluons, the symmetry factor $N(n,l) = l!(n-l-1)!$. For example,

processes $12 \to 3p$, $12 \to 34p$, $123 \to 4p$ yield $(n, l) = (4, 2), (5, 2), (5, 3)$ and $N(n, l) = 2, 4, 6$, respectively.

In vacuum, the matrix element squared for the 22 process is

$$|M_{12\to34}|^2 = \frac{9}{2}(4\pi)^2 N_g^2 \alpha_s^2 \left(3 - \frac{tu}{s^2} - \frac{su}{t^2} - \frac{st}{u^2}\right), \quad (6)$$

where $\alpha_s = g^2/(4\pi)$ is the strong coupling constant, and (s, t, u) are the Mandelstam variables $s = (p_1 + p_2)^2$, $t = (p_1 - p_3)^2$ and $u = (p_1 - p_4)^2$.

For the 23 process [53,54], under the convention $\sum_{i=1}^5 p_i = 0$, we have

$$\begin{aligned}|M_{12345\to0}|^2 &= |M_{0\to12345}|^2 \\ &= 54\pi^3 N_g^2 \alpha_s^3 [(12)^4 + (13)^4 + (14)^4 + (15)^4 \\ &\quad + (23)^4 + (24)^4 + (25)^4 + (34)^4 + (35)^4 \\ &\quad + (45)^4] \sum_{\text{perm}\{1,2,3,4,5\}} \frac{1}{(12)(23)(34)(45)(51)},\end{aligned} \quad (7)$$

where $(ij) \equiv p_i \cdot p_j$ and the sum is over all permutations of $\{1, 2, 3, 4, 5\}$. To convert to the convention $p_1 + p_2 = p_3 + p_4 + p_5$, we just perform the replacement:

$$\begin{aligned}|M_{12\to345}|^2 &= |M_{0\to12345}|^2|_{p_1\to-p_1, p_2\to-p_2}, \\ |M_{345\to12}|^2 &= |M_{12345\to0}|^2|_{p_1\to-p_1, p_2\to-p_2}.\end{aligned} \quad (8)$$

In the medium, the gluon thermal mass effect serves as the infrared (IR) cutoff to regularize IR sensitive observables. The most singular part of Eq. (6) comes from the collinear region (i.e., either $t \approx 0$ or $u \approx 0$), which can be regularized by the HTL corrections to the gluon propagators [55,56] and yields [57]

$$\begin{aligned}|M_{12\to34}|^2 &\approx \frac{1}{4}(12\pi\alpha_s)^2 N_g^2 (4E_1E_2)^2 \\ &\quad \times \left|\frac{1}{\mathbf{q}^2 + \Pi_L} - \frac{(1 - \bar{x}^2)\cos\phi}{\mathbf{q}^2(1 - \bar{x}^2) + \Pi_T}\right|^2,\end{aligned} \quad (9)$$

where $q = p_1 - p_3 = (q_0, \mathbf{q})$, $\bar{x} = q_0/|\mathbf{q}|$, and ϕ is the angle between $\hat{\mathbf{p}}_1 \times \hat{\mathbf{q}}$ and $\hat{\mathbf{p}}_2 \times \hat{\mathbf{q}}$. The HTL self-energies Π_L (longitudinal) and Π_T (transverse) are given by

$$\begin{aligned}\Pi_L &= m_D^2 \left[1 - \frac{\bar{x}}{2}\ln\frac{1 + \bar{x}}{1 - \bar{x}} + i\frac{\pi}{2}\bar{x}\right], \\ \Pi_T &= m_D^2 \left[\frac{\bar{x}^2}{2} + \frac{\bar{x}}{4}(1 - \bar{x}^2)\ln\frac{1 + \bar{x}}{1 - \bar{x}} - i\frac{\pi}{4}\bar{x}(1 - \bar{x}^2)\right].\end{aligned} \quad (10)$$

The external gluon mass m_∞ (i.e., the asymptotic mass) is the mass for an on-shell transverse gluon, and $m_\infty^2 = \Pi_T(|\bar{x}| = 1) = m_D^2/2$ both in the HTL approximation and in the full one-loop result.

Previous investigations of the thermodynamics within resummed perturbation theory showed that the most important plasma effects are the thermal masses $\sim gT$ acquired by the hard thermal particles [58–60]. So, a simpler (though less accurate) treatment for the regulator is to insert the Debye mass $m_D = (4\pi\alpha_s)^{1/2}T$ to the gluon propagator such that in the center-of-mass (CM) frame,

$$|M_{12\to34}|^2_{\text{CM}} \approx (12\pi\alpha_s)^2 N_g^2 \frac{s^2}{(\mathbf{q}_T^2 + m_D^2)^2}, \quad (11)$$

where $\mathbf{q}_T$ is the transverse component of $\mathbf{q}$ with respect to $\mathbf{p}_1$. It can be shown easily that Eqs. (9) and (11) coincide in the CM frame in vacuum. This treatment was used in Refs. [30,32,49]. We will show both results using HTL and m_D for the mass of the internal gluon propagators for comparison.

For the 23 process, because the matrix element is already quite complicated, we will just take m_D as the regulator for internal gluons and estimate the errors. In the $\sum_{i=1}^5 p_i = 0$ convention, one can easily show that an internal gluon will have a momentum of $\pm(p_i + p_j)$ rather than $\pm(p_i - p_j)$. Therefore, the gluon propagator factors (ij) in the denominator of Eq. (7), should be modified to

$$(ij) = \frac{1}{2}[(p_i + p_j)^2 - m_D^2] = p_i \cdot p_j + \frac{2m_g^2 - m_D^2}{2}, \quad (12)$$

where we use m_g to denote the external gluon mass. Then one applies Eq. (8) for the Boltzmann equation. In the numerator, the $(ij)^4$ combination is set by T and is $\mathcal{O}(T^8)$. So, we can still apply the substitution of Eq. (12), even if the (ij) factors might not have the inverse propagator form. The error is $\sim m_D^2(ij)^3 = \mathcal{O}(\alpha_s T^8)$, which is higher order in α_s.

It is instructive to show that Eqs. (7), (8), and (12) give the correct soft bremsstrahlung limit. Using the light-cone variable

$$p = (p^+, p^-, \mathbf{p}_\perp) \equiv (p_0 + p_3, p_0 - p_3, p_1, p_2), \quad (13)$$

we can rewrite one momentum configuration in the CM frame in terms of p, p', q, and k: $p_1 = p$, $p_2 = p'$, $p_3 = p + q - k$, $p_4 = p' - q$, and $p_5 = k$, with

$$\begin{aligned}&p = (\sqrt{s}, m_g^2/\sqrt{s}, 0, 0), \qquad p' = (m_g^2/\sqrt{s}, \sqrt{s}, 0, 0), \\ &k = (y\sqrt{s}, (k_\perp^2 + m_g^2)/y\sqrt{s}, k_\perp, 0), \qquad q = (q^+, q^-, q_\perp).\end{aligned} \quad (14)$$

The on-shell condition $p_3^2 = p_4^2 = m_g^2$ yields

$$\begin{aligned}q^+ &\simeq -q_\perp^2/\sqrt{s}, \\ q^- &\simeq \frac{k_\perp^2 + yq_\perp^2 - 2y\mathbf{k}_\perp \cdot \mathbf{q}_\perp + (1 - y + y^2)m_g^2}{y(1 - y)\sqrt{s}}.\end{aligned} \quad (15)$$

Taking the large s limit, then the $y \to 0$, we obtain

$$\begin{aligned}|M_{12\to345}|^2_{\text{CM}} &= \sum_{\text{perm}\{3,4,5\}} 3456\pi^3 N_g^2 \alpha_s^3 \\ &\quad \times \frac{s^2}{(k_\perp^2 + m_g^2)(q_\perp^2 + m_D^2)[(\mathbf{k}_\perp - \mathbf{q}_\perp)^2 + m_D^2]},\end{aligned} \quad (16)$$

where the permutation is over all final state gluon configurations. We see that Eq. (16) reduces to the Gunion-Bertsch

formula [61] after taking $m_D, m_g \to 0$. A similar derivation can be found in Ref. [62,63].

III. BEYOND VARIATION—SOLVING FOR η SYSTEMATICALLY

Following the standard procedure, the shear viscosity is related to $B(p)$ by

$$\eta = \frac{N_g}{10T}\int \frac{d^3p}{(2\pi)^3 E_p} f_p^{\rm eq}(1+f_p^{\rm eq})\left(\mathbf{p}^i\mathbf{p}^j - \frac{1}{3}\delta_{ij}\mathbf{p}^2\right)B_{ij}(p). \tag{17}$$

$B_{ij}(p)$ satisfies the constraint derived from the linearized Boltzmann equation,

$$\begin{aligned}\mathbf{p}^i\mathbf{p}^j - \frac{1}{3}\delta_{ij}\mathbf{p}^2 =& \frac{E_p}{2N_g}\int_{123} d\Gamma_{12\to 3p} f_1^{\rm eq} f_2^{\rm eq}(1+f_3^{\rm eq})(f_p^{\rm eq})^{-1}[B_{ij}(p)+B_{ij}(p_3)-B_{ij}(p_1)-B_{ij}(p_2)]\\ &+\frac{E_p}{4N_g}\int_{1234} d\Gamma_{12;34p}(1+f_1^{\rm eq})(1+f_2^{\rm eq}) f_3^{\rm eq} f_4^{\rm eq}(1+f_p^{\rm eq})^{-1}[B_{ij}(p)+B_{ij}(k_4)+B_{ij}(k_3)-B_{ij}(k_2)-B_{ij}(k_1)]\\ &+\frac{E_p}{6N_g}\int_{1234} d\Gamma_{123;4p}(1+f_1^{\rm eq})(1+f_2^{\rm eq})(1+f_3^{\rm eq}) f_4^{\rm eq}(1+f_p^{\rm eq})^{-1}[B_{ij}(p)+B_{ij}(k_4)-B_{ij}(k_3)-B_{ij}(k_2)-B_{ij}(k_1)].\end{aligned} \tag{18}$$

However, solving B_{ij} using this equation is technically challenging. It is easier to perform a projection (or convolution) to the above equation, then solve for the less restricted B_{ij}. We will discuss the procedure below.

By plugging Eq. (18) into Eq. (17), we obtain η in a bilinear form of B_{ij},

$$\begin{aligned}\eta =& \frac{1}{80T}\int\prod_{i=1}^{4}\frac{d^3k_i}{(2\pi)^3 2E_i}|M_{12\to 34}|^2(2\pi)^4\delta^4(k_1+k_2-k_3-k_4)(1+f_1^{\rm eq})(1+f_2^{\rm eq}) f_3^{\rm eq} f_4^{\rm eq}\\ &\times[B_{ij}(k_4)+B_{ij}(k_3)-B_{ij}(k_2)-B_{ij}(k_1)]^2\\ &+\frac{1}{120T}\int\prod_{i=1}^{5}\frac{d^3k_i}{(2\pi)^3 2E_i}|M_{12\to 345}|^2(2\pi)^4\delta^4(k_1+k_2-k_3-k_4-k_5)\\ &\times(1+f_1^{\rm eq})(1+f_2^{\rm eq}) f_3^{\rm eq} f_4^{\rm eq} f_5^{\rm eq}[B_{ij}(k_5)+B_{ij}(k_4)+B_{ij}(k_3)-B_{ij}(k_2)-B_{ij}(k_1)]^2.\end{aligned} \tag{19}$$

Then one can solve for B_{ij} which equates the right hand sides of Eqs. (17) and (19). This is nothing but a projection of Eq. (18). The resulting solution is not unique because only the projected equation, but not the equation itself, is satisfied. However, it is proven [28,64] that the true solution of B_{ij}, i.e. the solution satisfying Eq. (18), would give the maximum value of η. Thus, solving for η becomes a variational problem.

Recently, an algorithm is developed to find the true solution of B_{ij} systematically [65]. Thus, this approach is no more variational but systematic. Here we outline the procedure. First, expanding $B(p)$ using a specific set of orthogonal polynomials [41,42],

$$B(p) = (E_p/T)^y\sum_{r=0}^{r_{\max}} b_r B^{(r)}(E_p/T), \tag{20}$$

with y a constant chosen to be 1 in this case. The dimensionless polynomial $B^{(r)}$ satisfying the orthonormal condition

$$\int\frac{d^3p}{(2\pi)^3 E_p} f_p^{\rm eq}(1+f_p^{\rm eq})|\mathbf{p}|^2(E_p/T)^y B^{(r)}(E_p/T) \times B^{(s)}(E_p/T) = T^4\delta_{rs}. \tag{21}$$

Then Eq. (19) can be written in a compact form,

$$\eta = \langle B|F|B\rangle = \sum_{r,s=0}^{r_{\max}} b_r b_s\langle B^{(r)}|F|B^{(s)}\rangle, \tag{22}$$

while Eq. (17) gives

$$\begin{aligned}\eta =& \sum_{r=0}^{r_{\max}} b_r\frac{N_g}{15T}\int\frac{d^3p}{(2\pi)^3 E_p} f_p^{\rm eq}(1+f_p^{\rm eq})|\mathbf{p}|^2(E_p/T)^y B^{(r)}(E_p/T)\\ =& \sum_{r=0}^{r_{\max}} b_r L^{(r)}\delta_{r0} = b_0 L^{(0)},\end{aligned} \tag{23}$$

with

$$L^{(0)} = \frac{N_g}{15T}B^{(0)}\int\frac{d^3p}{(2\pi)^3 E_p} f_p^{\rm eq}(1+f_p^{\rm eq})|\mathbf{p}|^2(E_p/T)^y. \tag{24}$$

From Eqs. (22) and (23), we can find b_0 by solving the equation

$$L^{(r)}\delta_{r0} = \sum_{s=0}^{r_{\max}} b_s\langle B^{(r)}|F|B^{(s)}\rangle, \tag{25}$$

and then determine η from Eq. (23). [Note that there could be more than one solution satisfying Eqs. (22) and (23), but they all give the same η.]

In Ref. [65], it is proven that this procedure gives a monotonically increasing value of η with increasing $r_{\max}$. Thus, one can systematically approach the true value of η by adding more terms in the expansion of Eq. (20). We find good convergence in this algorithm. From $r_{\max} = 1$ to 2, η changes by less than 2% for $\alpha_s \leq 0.3$. Better convergence is found for smaller α_s.

IV. NUMERICAL RESULTS

A. Leading-Log result

The leading order $[O(\alpha_s^{-2})]$ contribution to η only involves the 22 and 23 processes [28]. The 22 collision rate is larger than 23 by a $(\ln\alpha_s)$ factor. In the leading-log (LL) approximation, one just needs to focus on the small q_T contribution from the 22 process. Furthermore, it was shown in [66,67] that using the HTL regulator (9) gives the same LL viscosity to that using the m_D regulator (11). Thus, after performing the small q_T expansion to Eq. (19), we obtain

$$\eta_{\rm LL} \simeq 27.1 \frac{T^3}{g^4 \ln(1/g)}, \tag{26}$$

which coincides with that of [27] to significant digits shown above. Using the entropy density for noninteracting gluons, $s = N_g \frac{2\pi^2}{45} T^3$ (for $m_g = 0$), we obtain

$$\frac{\eta_{\rm LL}}{s} \simeq \frac{3.9}{g^4 \ln(1/g)}. \tag{27}$$

This will be used to check our numerical result later.

η_{22}—Shear viscosity with the 22 process only

To study the effect of the HTL regulator, η_{22} (i.e., η with the 22 process only) with the HTL and m_D for the internal gluon masses, respectively, are shown in Fig. 1. The LL result $\eta_{\rm LL}$ and AMY's η_{22} [denoted as $\eta_{22(\rm AMY)}$] [27,28] are also shown. The external gluon mass m_g, used in kinematics and in $f_p^{\rm eq}$ such that $E_p = \sqrt{\mathbf{p}^2 + m_g^2}$, is a higher order effect in η_{22}. Changing m_g from 0 to $m_D = \sqrt{2} m_\infty$ yields an $O(m_\infty^2/T^2) = O(\alpha_s)$ variation to η_{22}. This is confirmed numerically in the left panel of Fig. 1. It is a good check to our numerical calculation that $\eta_{22(\rm HTL)}$ and $\eta_{22(\rm MD)}$ both converge to $\eta_{\rm LL}$ in small α_s, and $\eta_{22(\rm HTL)}$ agrees well with $\eta_{22(\rm AMY)}$ when $m_g = 0$ is used to conform with the AMY result.

About the HTL effect, $\eta_{22(\rm HTL)}/\eta_{22(\rm MD)}$ is quite close to unity at $\alpha_s = 10^{-6}$, see the right panel of Fig. 1. This ratio gets smaller at larger α_s and reaches 0.65 at $\alpha_s = 0.1$ with little m_g dependence (each $\eta_{22(\rm HTL)}/\eta_{22(\rm MD)}$ is evaluated with the same m_g). This means the error is $\sim$30% in the shear viscosity at $\alpha_s = 0.1$ if we use m_D as the regulator for the gluon propagator instead of the HTL propagator.

C. η_{22+23}—Shear viscosity with the 22 and 23 processes

In our full calculation, we use the HTL propagator for the 22 process. However, for technical reasons, we use the internal gluon mass m_D for the 23 process. More specifically, we use matrix elements of Eqs. (7)–(9) and (12), $E_p = \sqrt{\mathbf{p}^2 + m_g^2}$ in kinematics and $f_p^{\rm eq}$ for external gluons, and $m_g = m_\infty$. If the external gluons are massless but the internal gluons are massive, then the $1/[(p_1 + p_2)^2 - m_D^2]$ factor could diverge. Using $m_g = m_\infty$, each term in Eq. (7) is non-negative. In AMY and XG, external gluon masses were not included ($m_g = 0$). This divergence was avoided by keeping only the most singular matrix elements in the small $k_\perp$, $q_\perp$ limit, and taking the collinear approximation (AMY) or regulating the gluon bremsstrahlung infrared divergence by the Landau-Pomeranchuk-Migdal (LPM) effect (XG) which will be discussed in Sec. IV D.

We show η_{22}/s and η_{22+23}/s in the left panel of Fig. 2, where the HTL propagator is used for 22 and the external

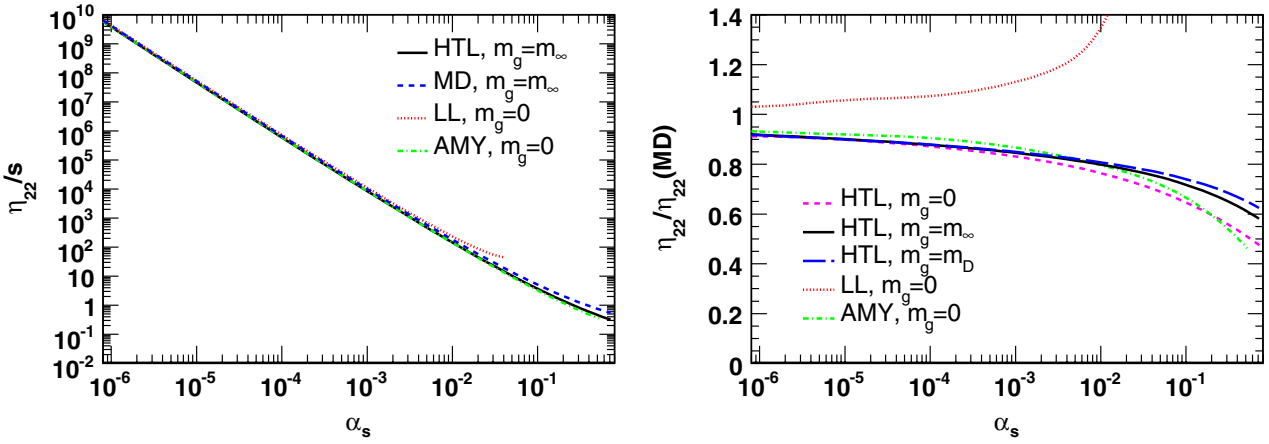

FIG. 1 (color online). η_{22} over the entropy density (left panel) and η_{22} over $\eta_{22(\rm MD)}$ (right panel) in various treatments. "LL" is the leading-log result of Eq. (26). "HTL" is the result using the full HTL matrix element of Eq. (9). "MD" is the result using m_D as the regulator as in Eq. (11). "AMY" is AMY's result.

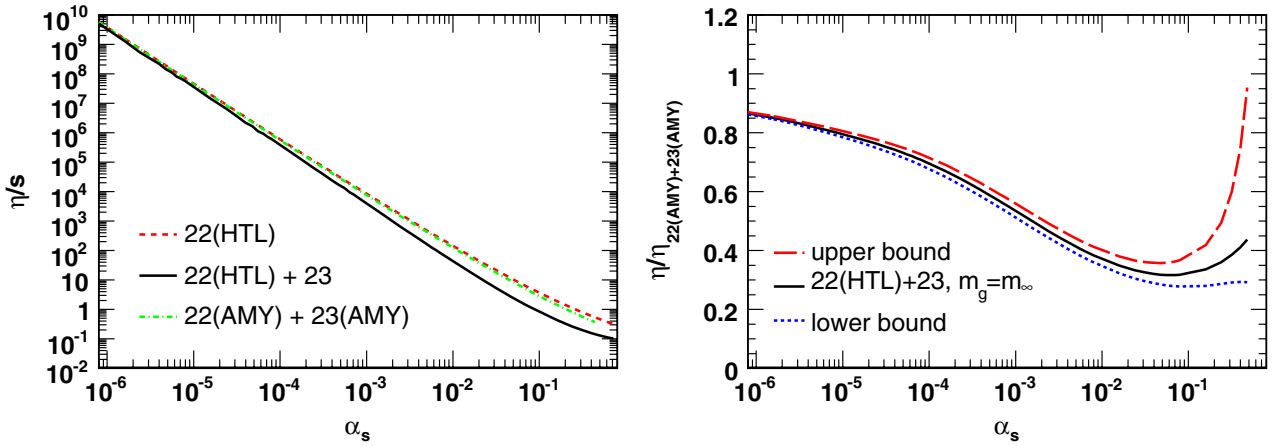

FIG. 2 (color online). Left panel: η_{22}/s and η_{22+23}/s for various cases. Right panel: the ratio of our result to AMY's. '22(HTL) + 23' denotes η_{22+23} where $m_g = m_\infty$, the full HTL matrix element (9) is used for the 22 process, and the matrix elements of Eqs. (7)–(9) and (12) are used for the 23 process. '22(AMY) + 23(AMY)' denotes AMY's result for η_{22+23} ($m_g = 0$). The range of the "recommended value" of η_{22+23} is bounded by η_-(lower bound) and η_+(upper bound).

gluon mass $m_g = m_\infty$. We also show AMY's result for η_{22+23}/s for comparison. In the right panel of Fig. 2, we see that the ratio of our result to AMY's approaches unity at very small α_s and $\sim$0.5 at $\alpha_s \approx 0.001$. The deviation in moderate α_s is partly due to the finite angle, noncollinear 3-body configurations in the 23 process described by the full matrix element (7) and partly due to the gluon mass. We have also included a theoretical error band for η_{22+23} which will be discussed in Section IV D.

The effect of the 23 process can be seen more clearly in the ratio η_{22+23}/η_{22} shown in Fig. 3. We have plotted $\eta_{22(\mathrm{HTL})+23}/\eta_{22(\mathrm{HTL})}$ together with AMY's and XG's result for comparison. The 22 process dominates at small α_s. When α_s increases, η_{22+23}/η_{22} decreases and the central value reaches the minimum of $\sim$0.25 (which means the 23 collision rate is $\sim$3 times of 22!) at $\alpha_s \simeq 0.1$ and then increases again for $\alpha_s \gtrsim 0.1$.

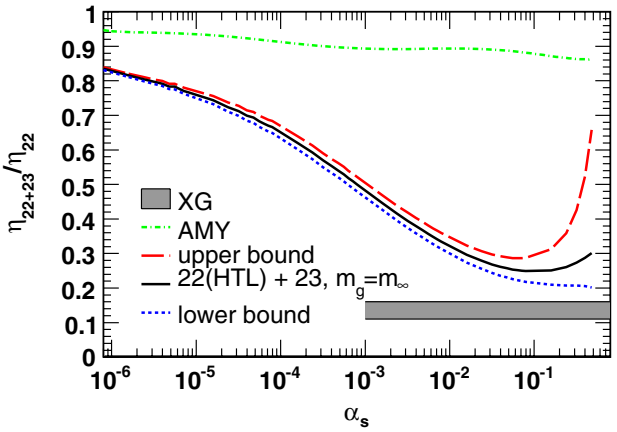

FIG. 3 (color online). η_{22+23}/η_{22} in various cases. "22 (HTL)" uses HTL gluon propagators for the 22 process. The range of the "recommended value" of η_{22+23} is bounded by η_-(lower bound) and η_+(upper bound). The external gluon mass is set to m_∞. AMY's and XG's η_{22+23}/η_{22} are also shown.

We see that AMY's result which employs the collinear approximation for the $1 \leftrightarrow 2$ process (corresponding to our 23 process), gives η_{22+23}/η_{22} close to unity. This implies their 23 collisions is just a small perturbation to the 22 collisions. XG's result, which employs the soft gluon bremsstrahlung approximation, however, gives $\eta_{22+23}/\eta_{22} \simeq [0.11, 0.16]$ around 1/8. This implies their 23 collision rate is about 7 times bigger than the 22 collision rate. Our result, which takes neither of the approximations, lies between AMY's and XG's results and between two previous calculations with different approximations to the phase space [32]. Furthermore, our result smoothly connects the two different approximations used by AMY and XG: at small α_s ($\alpha_s \ll 1$), our result is closer to AMY's collinear result while at larger α_s, the finite angle noncollinear configuration becomes more important and our result is qualitatively closer to XG's soft bremsstrahlung result.

D. Error estimation

Our $\eta_{22(\mathrm{HTL})+23}/s$ is tabulated in Table I. The error assignment is based on the following error analyses for η_{22+23}:

(a) HTL corrections for the 23 process. From our η_{22} error analysis, we assign a $\sim$30% error at $\alpha_s = 0.1$ to the 23 contribution for not implementing the HTL approach to the 23 collisions. The error will be smaller at smaller α_s if the scaling for η_{22} holds also for the error. Since the HTL effect tends to reduce the magnetic screening effect which lowers the IR cut-off and enhances the 23 collision rate, the HTL correction tends to reduce η_{22+23}.

(b) LPM effect. We will try to estimate the error from neglecting the LPM effect. An intuitive explanation of this effect is given in Ref. [68]: for the soft bremsstrahlung gluon with transverse momentum k_T, the mother gluon has a transverse momentum uncertainty $\sim k_T$ and a size uncertainty $\sim 1/k_T$. It takes the bremsstrahlung gluon the formation time $t \sim 1/(k_T v_T) \sim E_k/k_T^2$ to fly far enough from the mother gluon to be resolved as a radiation. But if the formation time is longer than the mean free path $l_{\rm mfp} \approx O(\alpha_s^{-1})$, then the radiation is incomplete and it would be resolved as $gg \to gg$ instead of $gg \to ggg$. Thus, the resolution scale is set by $t \le l_{\rm mfp}$. This yields an IR cutoff $k_T^2 \ge E_k/l_{\rm mfp} \approx O(\alpha_s)$ on the phase space [69]. Thus, the LPM effect reduces the 23 collision rate and will increase η_{22+23}. Our previous calculation using the Gunion-Bertsch formula shows that implementing the m_D regulator gives a very close result to the LPM effect [32]. Thus, we will estimate the size of the LPM effect by increasing the external gluon mass m_g from m_∞ to m_D.

(c) Higher order effect. The higher order effect is parametrically suppressed by $O(\alpha_s)$, but the size is unknown. Computing this effect requires a treatment beyond the Boltzmann equation [37] and the inclusion of the 33 and 24 processes. We just estimate the effect to be α_s times the leading order, which is $\sim 10\%$ at $\alpha_s = 0.1$.

Combining the above analyses, we consider errors from (a) to (c). To compute a recommended range for η/s, we will work with the R_{22} and R_{23} collision rates defined as

$$R_{22}^{-1} \equiv \eta_{22(\rm HTL)}, \quad (R_{22} + R_{23})^{-1} \equiv \eta_{22(\rm HTL)+23}. \tag{28}$$

Using HTL instead of m_D in for the gluon propagator enhances the 22 rate by a factor of

$$\delta \equiv \frac{R_{22(\rm HTL)}}{R_{22(\rm MD)}} = \frac{\eta_{22(\rm MD)}}{\eta_{22(\rm HTL)}}. \tag{29}$$

We will assume that the same enhancement factor appears in the 23 rate as well, such that

$$\delta \simeq \frac{R_{23(\rm HTL)}}{R_{23(\rm MD)}}. \tag{30}$$

On the other hand, the LPM effect is estimated to suppress the 23 rate by a factor of

$$\gamma = \frac{R_{23}(m_g = m_D)}{R_{23}(m_g = m_\infty)}. \tag{31}$$

Combining the estimated HTL and LPM corrections to the 23 rate, the $22 + 23$ rate is likely to lie in the range $[R_{22} + R_{23}, R_{22} + \gamma\delta R_{23}]$, while the higher order effect gives $\pm\alpha_s(R_{22} + R_{23})$ corrections to the rate. Without

TABLE I. η/s values for our $\eta_{22(\rm HTL)+23}/s$ result and the range of our "recommended values" bounded by η_-/s and η_+/s.

α_s	$\frac{\eta_{22(\rm HTL)+23}}{s}$	$\frac{\eta_-}{s}$	$\frac{\eta_+}{s}$	α_s	$\frac{\eta_{22(\rm HTL)+23}}{s}$	$\frac{\eta_-}{s}$	$\frac{\eta_+}{s}$
0.100 E-5	0.316 E10	0.315 E10	0.318 E10	0.100	0.914	0.790	1.07
0.158 E-5	0.129 E10	0.128 E10	0.130 E10	0.125	0.666	0.567	0.801
0.251 E-5	0.524 E9	0.520 E9	0.528 E9	0.150	0.520	0.436	0.642
0.398 E-5	0.213 E9	0.212 E9	0.215 E9	0.175	0.426	0.352	0.540
0.631 E-5	0.870 E8	0.860 E8	0.879 E8	0.200	0.361	0.294	0.471
0.100 E-4	0.354 E8	0.350 E8	0.359 E8	0.225	0.313	0.252	0.423
0.158 E-4	0.144 E8	0.142 E8	0.147 E8	0.250	0.278	0.220	0.388
0.251 E-4	0.586 E7	0.575 E7	0.597 E7	0.275	0.250	0.194	0.362
0.398 E-4	0.238 E7	0.233 E7	0.243 E7	0.300	0.228	0.174	0.344
0.631 E-4	0.965 E6	0.941 E6	0.989 E6	0.325	0.210	0.158	0.331
0.100 E-3	0.390 E6	0.380 E6	0.401 E6	0.350	0.195	0.144	0.322
0.158 E-3	0.157 E6	0.153 E6	0.162 E6	0.375	0.183	0.133	0.316
0.251 E-3	0.634 E5	0.613 E5	0.656 E5	0.400	0.172	0.123	0.314
0.398 E-3	0.255 E5	0.246 E5	0.265 E5	0.425	0.163	0.114	0.314
0.631 E-3	0.102 E5	0.985 E4	0.107 E5	0.450	0.155	0.106	0.317
0.100 E-2	0.411 E4	0.394 E4	0.430 E4	0.475	0.148	0.995 E-1	0.322
0.158 E-2	0.165 E4	0.158 E4	0.174 E4	0.500	0.142	0.934 E-1	0.329
0.251 E-2	668.	635.	706.	0.525	0.137	0.879 E-1	0.338
0.398 E-2	272.	257.	289.	0.550	0.132	0.828 E-1	0.349
0.631 E-2	112.	105.	119.	0.575	0.128	0.781 E-1	0.363
0.100 E-1	46.5	43.4	50.2	0.600	0.124	0.738 E-1	0.379
0.158 E-1	19.8	18.3	21.5	0.625	0.121	0.698 E-1	0.397
0.251 E-1	8.64	7.90	9.51	0.650	0.118	0.660 E-1	0.418
0.398 E-1	3.90	3.52	4.36	0.675	0.115	0.624 E-1	0.441
0.631 E-1	1.84	1.63	2.10	0.700	0.112	0.590 E-1	0.467

further information, the errors are assumed to be Gaussian and uncorrelated, the total rate is

$$\left(R_{22}+\frac{\gamma\delta+1}{2}R_{23}\right)\pm\left(\frac{\gamma\delta-1}{2}R_{23}\right)\pm\alpha_s(R_{22}+R_{23}), \tag{32}$$

and the recommended upper (η_+) and lower (η_-) ranges for η_{22+23} are

$$\eta_\pm=\frac{1}{(R_{22}+\frac{\gamma\delta+1}{2}R_{23})\mp\sqrt{(\frac{\gamma\delta-1}{2}R_{23})^2+\alpha_s^2(R_{22}+R_{23})^2}}. \tag{33}$$

The $\eta_\pm$ values are shown in the right panel of Fig. 2 and in Fig. 3.

Our final η/s result is as presented in Table I. At $\alpha_s=0.1$, $\eta/s\simeq[0.79, 1.07]$, which is between 2.5 of AMY and 0.5 of XG. At $\alpha_s=0.3$ and 0.6, we have $\eta/s\simeq[0.17, 0.34]$ and $[0.074, 0.38]$, respectively, whose lower bounds are close to 0.13 and 0.076 obtained by XG.

E. When does the α_s perturbation break down?

We have only carried out the LO $[O(\alpha_s^{-2})]$ η/s in the α_s expansion. Without computing the higher order contribution, it is hard to tell at what value of α_s the perturbation starts to break down. In the above section, we have naively assumed the higher order contribution to be the leading order times α_s, i.e. the expansion breaks down at $\alpha_s\simeq 1$. However, explicit computations of thermal dynamical quantities and transport coefficients showed that the breakdown might happen at smaller α_s [58–60] (the screening mass computation breaks down at $\alpha_s\simeq 0.1$ [59] and the heavy quark diffusion constant computation breaks down at $\alpha_s\simeq 0.01$[60]).

Looking more closely to our LO η/s shown in the left panel of Fig. 2, the α_s dependence of η/s changes qualitatively at $\alpha_s\simeq 0.1$. This could be a sign that higher order α_s dependence has become as important as the LO one. Thus, the higher order corrections could be bigger than our previous estimation, and our result might be only reliable when $\alpha_s\lesssim 0.1$.

Having said that, it is interesting that our η/s bends slightly upward at $\alpha_s\gtrsim 0.1$ as if η/s is trying to avoid going below the conjectured $1/4\pi$ bound. Also, our result can smoothly connect to the lattice result in the nonperturbative region. Several models have proposed to describe the microscopic picture in the nonperturbative region [70–73], and a similar result to ours is obtained in a recent calculation [74] based on one kind of simplification of the 23 matrix element [62].

Can the proposed perfect fluid limit $\eta/s\simeq 1/(4\pi)$ be achieved by perturbative QCD alone? In the region where perturbation is reliable ($\alpha_s\lesssim 0.1$), we do not find support for this. Whether this can be achieved for $\alpha_s\gtrsim 0.1$ (the values of practical interests) is still an open question.

V. CONCLUSIONS

We have calculated the LO $[O(\alpha_s^{-2})]$ η/s of a gluon plasma in perturbation using the kinetic theory. The LO contribution only involves the 22 and 23 processes. The HTL propagator has been used for the 22 matrix element, while the exact matrix element in vacuum is supplemented by the Debye mass m_D for gluon propagators for the 23 process. The asymptotic mass $m_\infty=m_D/\sqrt{2}$ is used for the external gluon mass in the kinetic theory, as well. The errors from not implementing HTL and the LPM effect in the 23 process, and from the uncalculated higher order $[O(\alpha_s^{-1})]$ corrections, have been estimated.

Our result smoothly connects the two different approximations used by AMY and XG. At small α_s ($\alpha_s\ll 1$), our result is closer to AMY's collinear result, while at larger α_s the finite angle noncollinear configurations become more important and our result is closer to XG's soft bremsstrahlung result.

In the region where perturbation is reliable ($\alpha_s\lesssim 0.1$), we find no indication that the proposed perfect fluid limit $\eta/s\simeq 1/(4\pi)$ can be achieved by perturbative QCD alone. Whether this can be achieved for $\alpha_s\gtrsim 0.1$ (the values of practical interests) is still an open question.

ACKNOWLEDGMENTS

We thank G. Moore for providing us their tables of η/s. J. W. C. and Q. W. thank KITPC, Beijing, for hospitality. J. W. C. is supported by the NSC and NCTS of ROC. Q. W. is supported in part by the "100 talents" project of Chinese Academy of Sciences and by the National Natural Science Foundation of China under Grant No. 10735040. H. D. is supported in part by the Natural Science Foundation of the Shandong province under Grant No. ZR2010AQ008. J. D. is supported in part by the Innovation Foundation of Shandong University under Grant No. 2010GN031.

[1] J. M. Maldacena, Adv. Theor. Math. Phys. **2**, 231 (1998); Int. J. Theor. Phys. **38**, 1113 (1999).
[2] S. S. Gubser, I. R. Klebanov, and A. M. Polyakov, Phys. Lett. B **428**, 105 (1998).
[3] E. Witten, Adv. Theor. Math. Phys. **2**, 253 (1998).
[4] A. Buchel and J. T. Liu, Phys. Rev. Lett. **93**, 090602 (2004).

[5] P. Kovtun, D. T. Son, and A. O. Starinets, Phys. Rev. Lett. **94**, 111601 (2005).
[6] A. Buchel, Phys. Lett. B **609**, 392 (2005).
[7] T. D. Cohen, Phys. Rev. Lett. **99**, 021602 (2007).
[8] A. Cherman, T. D. Cohen, and P. M. Hohler, J. High Energy Phys. 02 (2008) 026.
[9] Y. Kats and P. Petrov, J. High Energy Phys. 01 (2009) 044.
[10] M. Brigante, H. Liu, R. C. Myers, S. Shenker, and S. Yaida, Phys. Rev. D **77**, 126006 (2008).
[11] M. Brigante, H. Liu, R. C. Myers, S. Shenker, and S. Yaida, Phys. Rev. Lett. **100**, 191601 (2008).
[12] A. Buchel, R. C. Myers, and A. Sinha, J. High Energy Phys. 03 (2009) 084.
[13] J. I. Kapusta, arXiv:0809.3746.
[14] T. Schafer and D. Teaney, Rep. Prog. Phys. **72**, 126001 (2009).
[15] I. Arsene *et al.* (BRAHMS Collaboration), Nucl. Phys. **A757**, 1 (2005).
[16] B. B. Back *et al.*, Nucl. Phys. **A757**, 28 (2005).
[17] K. Adcox *et al.* (PHENIX Collaboration), Nucl. Phys. **A757**, 184 (2005).
[18] M. Luzum and P. Romatschke, Phys. Rev. C **78**, 034915 (2008).
[19] H. Song and U. W. Heinz, J. Phys. G **36**, 064033 (2009).
[20] H. B. Meyer, Phys. Rev. D **76**, 101701 (2007).
[21] T. Schafer, Phys. Rev. A **76**, 063618 (2007).
[22] A. Turlapov, J. Kinast, B. Clancy, L. Luo, J. Joseph, and J. E. Thomas, J. Low Temp. Phys. **150**, 567 (2007).
[23] B. Clancy, L. Luo, and J. E. Thomas, Phys. Rev. Lett. **99**, 140401 (2007).
[24] J. E. Thomas, Nucl. Phys. **A830**, 665c (2009).
[25] T. Schaefer and C. Chafin, arXiv:0912.4236.
[26] T. Schaefer, arXiv:1008.3876.
[27] P. Arnold, G. D. Moore, and L. G. Yaffe, J. High Energy Phys. 11 (2000) 001.
[28] P. Arnold, G. D. Moore, and L. G. Yaffe, J. High Energy Phys. 05 (2003) 051.
[29] P. Arnold, Int. J. Mod. Phys. E **16**, 2555 (2007).
[30] Z. Xu and C. Greiner, Phys. Rev. Lett. **100**, 172301 (2008).
[31] Z. Xu and C. Greiner, Phys. Rev. C **71**, 064901 (2005).
[32] J. W. Chen, H. Dong, K. Ohnishi, and Q. Wang, Phys. Lett. B **685**, 277 (2010).
[33] S. Jeon, Phys. Rev. D **52**, 3591 (1995).
[34] S. Jeon and L. G. Yaffe, Phys. Rev. D **53**, 5799 (1996).
[35] M. E. Carrington, D. f. Hou, and R. Kobes, Phys. Rev. D **62**, 025010 (2000).
[36] E. Wang and U. W. Heinz, Phys. Lett. B **471**, 208 (1999).
[37] Y. Hidaka and T. Kunihiro, arXiv:1009.5154.
[38] J. S. Gagnon and S. Jeon, Phys. Rev. D **76**, 105019 (2007).
[39] M. Prakash, M. Prakash, R. Venugopalan, and G. Welke, Phys. Rep. **227**, 321 (1993).
[40] A. Dobado and F. J. Llanes-Estrada, Phys. Rev. D **69**, 116004 (2004).
[41] A. Dobado and S. N. Santalla, Phys. Rev. D **65**, 096011 (2002).
[42] J. W. Chen and E. Nakano, Phys. Lett. B **647**, 371 (2007).
[43] J. W. Chen, Y. H. Li, Y. F. Liu, and E. Nakano, Phys. Rev. D **76**, 114011 (2007).
[44] K. Itakura, O. Morimatsu, and H. Otomo, Phys. Rev. D **77**, 014014 (2008).
[45] G. D. Moore, Phys. Rev. D **76**, 107702 (2007).
[46] J. W. Chen, M. Huang, Y. H. Li, E. Nakano, and D. L. Yang, Phys. Lett. B **670**, 18 (2008).
[47] U. W. Heinz, Ann. Phys. **161**, 48 (1985).
[48] H. T. Elze, M. Gyulassy, and D. Vasak, Nucl. Phys. **B276**, 706 (1986).
[49] T. S. Biro, E. van Doorn, B. Muller, M. H. Thoma, and X. N. Wang, Phys. Rev. C **48**, 1275 (1993).
[50] J. P. Blaizot and E. Iancu, Nucl. Phys. **B557**, 183 (1999).
[51] R. Baier, A. H. Mueller, D. Schiff, and D. T. Son, Phys. Lett. B **502**, 51 (2001).
[52] Q. Wang, K. Redlich, H. Stoecker, and W. Greiner, Phys. Rev. Lett. **88**, 132303 (2002).
[53] R. K. Ellis and J. C. Sexton, Nucl. Phys. **B269**, 445 (1986).
[54] T. Gottschalk and D. W. Sivers, Phys. Rev. D **21**, 102 (1980).
[55] H. A. Weldon, Phys. Rev. D **26**, 1394 (1982).
[56] R. D. Pisarski, Phys. Rev. Lett. **63**, 1129 (1989).
[57] H. Heiselberg and X. N. Wang, Nucl. Phys. **B462**, 389 (1996).
[58] J. P. Blaizot, E. Iancu, and A. Rebhan, Phys. Rev. D **63**, 065003 (2001).
[59] J. O. Andersen, E. Braaten, E. Petitgirard, and M. Strickland, Phys. Rev. D **66**, 085016 (2002).
[60] S. Caron-Huot and G. D. Moore, Phys. Rev. Lett. **100**, 052301 (2008).
[61] J. F. Gunion and G. Bertsch, Phys. Rev. D **25**, 746 (1982).
[62] S. K. Das and J. e. Alam, Phys. Rev. D **82**, 051502 (2010).
[63] R. Abir, C. Greiner, M. Martinez, and M. G. Mustafa, arXiv:1011.4638.
[64] P. Résibois and M. d. Leener, *Classical Kinetic Theory of Fluids* (John Wiley & Sons, New York, 1977).
[65] J. W. Chen, M. Huang, C. T. Hsieh, and H. H. Lin, arXiv:1010.3121.
[66] G. Baym, H. Monien, C. J. Pethick, and D. G. Ravenhall, Phys. Rev. Lett. **64**, 1867 (1990).
[67] H. Heiselberg, Phys. Rev. D **49**, 4739 (1994).
[68] M. Gyulassy, M. Plumer, M. Thoma, and X. N. Wang, Nucl. Phys. **A538**, 37 (1992).
[69] X. N. Wang, M. Gyulassy, and M. Plumer, Phys. Rev. D **51**, 3436 (1995).
[70] M. Asakawa, S. A. Bass, and B. Muller, Phys. Rev. Lett. **96**, 252301 (2006).
[71] Y. Hidaka and R. D. Pisarski, Phys. Rev. D **81**, 076002 (2010).
[72] A. S. Khvorostukhin, V. D. Toneev, and D. N. Voskresensky, arXiv:1011.0839.
[73] M. Bluhm, B. Kampfer, and K. Redlich, arXiv:1012.0488.
[74] S. K. Das and J. e. Alam, arXiv:1011.4181.